Int. J. Heat Mass Transfer. Vol. 35, No. 10, pp. 2717–2724, 1992
Printed in Great Britain

0017–9310/92 $5.00+0.00
Pergamon Press Ltd

Validation of a k–ε model based on experimental results in a thermally stable stratified turbulent boundary layer

R. MOREL,† A. LAASSIBI,† E. ALCARAZ,† R. ZEGADI,† G. BRUN‡ and D. JEANDEL†

†Laboratoire de Mécanique des Fluides et d'Acoustique, URA C.N.R.S. 263, Ecole Centrale de Lyon, B.P. 163-69131 Ecully Cedex, France.

‡Metraflu 64, chemin des Mouilles -69134 Ecully Cedex, France

(*Received* 28 *March* 1991 *and in final form* 30 *September* 1991)

Abstract—A 2D (k–ε) turbulence model was developed for use with dilatable flows at high Reynolds numbers. A new approach relative to the modelling of the density–velocity correlation term is proposed, and a relation concerning the Prandtl turbulent number was used taking into account both the wall and gravity effects. This model was validated by experimental results obtained at the E.C.L. Fluid Mechanics and Acoustics laboratory on a stable thermally stratified turbulent boundary layer developing at a quickly cooled smooth boundary surface.

1. INTRODUCTION

THE STUDY of flows in the presence of gravity effects is a subject that has been widely studied in the scientific community [1–7]. This interest is justified particularly by the impact of pollutant disposals on our environment. Flows involved in this type of problem are generally turbulent and may be the source of large temperature variations; they are then necessarily subjected to the effects of gravity. A detailed experimental approach to these situations is necessary in order to better understand transport or dispersion mechanisms involved. In this respect, it can refine physical models normally used. These models are generally based on statistical approaches to turbulence with one point closure model. The well-known k–ε two equations model is based on a turbulent viscosity assumption. However, this assumption does not appear to be suitable for taking into account the gravity effects which change the isotropic nature of this viscosity.

Modifications to this model are proposed here, making use of information obtained from more precise models (second order algebraic models) and experimental data obtained from stable stratified boundary layer experiments carried out in the laboratory. Modelling assumptions are described below followed by the experimental set up and comparisons between experimental and calculated results.

2. THE SYSTEM OF EQUATIONS

2.1. *Conservation equations*

The study described below applies to a low Mach number turbulent flow of a single phase fluid which may be the source of large temperature variations. The fluid density is then directly related to the temperature by a perfect gas state equation in which the pressure is assumed to be constant.

The statistical approach used is based on the Favre classical decomposition for temperature ($T = \bar{\bar{T}} + \theta''$), velocity $\left(\vec{U} = \vec{\bar{U}} + \vec{u}''\right)$ and the Reynolds decomposition for pressure ($P = \bar{P} + p'$) and density ($\rho = \bar{\rho} + \rho'$).

Neglecting radiation effects and variations of physical fluid properties, the state and conservation equations can be written as follows in dimensional form:

$$\frac{\partial \bar{\rho}}{\partial t} + \operatorname{div}\left(\bar{\rho}\vec{\bar{U}}\right) = 0$$

$$\frac{\partial}{\partial t}\bar{\rho}\vec{\bar{U}} + \operatorname{div}\left(\bar{\rho}\vec{\bar{U}} * \vec{\bar{U}}\right) = -\overrightarrow{\operatorname{grad}}\,\bar{P} + \operatorname{div}\bar{\bar{\tau}} - \operatorname{div}\left(\overline{\overline{\rho\vec{u}'' * \vec{u}''}}\right) + \bar{\rho}\cdot\vec{g}$$

$$\bar{\rho}\cdot C_p\left[\frac{\partial \bar{\bar{T}}}{\partial t} + \vec{\bar{U}}\,\overrightarrow{\operatorname{grad}}\,\bar{\bar{T}}\right] = \operatorname{div}\left[\lambda\,\overrightarrow{\operatorname{grad}}\,\bar{T}\right] - C_p\cdot\operatorname{div}\left(\overline{\overline{\rho\vec{u}''\theta''}}\right) + \left(\vec{\bar{U}} + \vec{u}''\right)\overrightarrow{\operatorname{grad}}\,\bar{P} + \frac{\partial \bar{P}}{\partial t} + \overrightarrow{\vec{u}''\,\overrightarrow{\operatorname{grad}}\,p'} + \bar{\varphi}$$

$$\bar{\rho}\,\bar{\bar{T}} = Cst$$

with $\bar{\bar{\tau}} = \mu\cdot\left[-\left(\frac{2}{3}\operatorname{div}\vec{U}\right)\cdot\bar{\bar{I}} + \left(\overrightarrow{\operatorname{grad}}\,\vec{U} + \overrightarrow{\operatorname{grad}^t}\,\vec{U}\right)\right]$

and

$$\bar{\varphi} = \overline{\bar{\bar{\tau}}\cdot\overrightarrow{\operatorname{grad}}\,\vec{U}}.$$

NOMENCLATURE

C sound celerity
C_p specific heat of air at constant pressure
C_v specific heat of air at constant volume
g acceleration of gravity
k turbulent kinetic energy per unity of mass, $\frac{1}{2}(\overline{u''^2}+\overline{v''^2}+\overline{w''^2})$
T_e external temperature flow
T_p wall temperature
U_* friction velocity, $(\tau_0/\rho)^{1/2}$
U_e external velocity flow
U, V and W longitudinal, lateral and vertical components of the flow
X, Y and Z longitudinal, lateral and vertical coordinates.

Greek symbols
β volumetric expansion coefficient
γ C_p/C_v
δ boundary layer thickness
ε rate of dissipation of turbulent kinetic energy
λ thermal conductivity
μ dynamic viscosity
ρ_e external density flow
τ_0 surface shearing stress.

2.2. *The k–ε model*

As the above system of equations is opened, the Reynolds tensor and the turbulent heat flux should be modelled.

This is done by using the Boussinesq hypothesis extended to flow with variable density [8] for the Reynolds tensor

$$\overline{\rho\vec{u}''*\vec{u}''} = \frac{2}{3}\left(\bar{\rho}k+\mu_t \operatorname{div}\vec{\bar{U}}\right)\cdot\bar{\bar{I}} - \mu_t\left(\overrightarrow{\operatorname{grad}}\,\vec{\bar{U}}+\overrightarrow{\operatorname{grad}}^t\,\vec{\bar{U}}\right)$$

and a first gradient assumption for heat fluxes [8]

$$-\overline{\rho\vec{u}''\theta''} = \frac{\mu_t}{Prt}\overrightarrow{\operatorname{grad}}\,\bar{T}.$$

The turbulent viscosity μ_t is a scalar quantity which can be linked to k and ε by the following relation [9]:

$$\mu_t = \bar{\rho}C_\mu\frac{k^2}{\varepsilon}.$$

The exact equation for the evolution of k may be obtained classically (see refs. [10, 11])

$$\frac{\partial}{\partial t}(\bar{\rho}k)+\operatorname{div}\left(\bar{\rho}\vec{\bar{U}}k\right) = \overbrace{-\overline{\rho\vec{u}''*\vec{u}''}:\overrightarrow{\operatorname{grad}}\,\vec{\bar{U}}}^{\bar{\rho}\cdot P_k} - \operatorname{div}\left[\overline{\rho\vec{u}''k}+\bar{\rho}\frac{\overline{\vec{u}''p'}}{\rho}+\overline{\vec{\tau}\cdot\vec{u}''}\right] \overbrace{-\vec{u}''\cdot\overrightarrow{\operatorname{grad}}\,\bar{P}}^{G_k}+p'\operatorname{div}\vec{u}''-\bar{\rho}\cdot\varepsilon.$$

This equation contains many unknown terms already encountered in incompressible flows or in flows at variable density. Classical models for incompressible fluids are extended to the dilatable case. The compressible case involves mixed density–velocity terms of the $\vec{u}''\cdot\overrightarrow{\operatorname{grad}}\,P$ type and dissipation terms due to viscous friction, of the form $\operatorname{div}\left(\overline{\vec{\tau}\cdot\vec{u}''}\right)$. The dissipation term $\bar{\rho}\cdot\varepsilon$ includes terms which are not present in the incompressible case; the equation for the evolution of this dissipation is much more difficult to handle than for the incompressible case and models used are normally based on those defined for incompressible fluids; this evolution equation is written in the form [11]

$$\frac{\partial\bar{\rho}\varepsilon}{\partial t}+\operatorname{div}\left(\bar{\rho}\cdot\vec{\bar{U}}\cdot\varepsilon\right) = -\operatorname{div}\left(\overline{\rho\cdot\vec{U}\cdot\varepsilon^i}\right)+\bar{\rho}\cdot(P_\varepsilon-D_\varepsilon)$$

where ε^i is the instantaneous dissipation, P_ε, D_ε are respectively the production of mean flow and dissipation by viscous effects.

2.3. *Modelling the density–velocity term*

The density–velocity correlation term appearing in the equation for the evolution of k can be written in the form

$$G_k = -\vec{u}''\overrightarrow{\operatorname{grad}}\,\bar{P} = \frac{\overline{\rho'\vec{u}''}}{\bar{\rho}}\overrightarrow{\operatorname{grad}}\,\bar{P}.$$

The problem is then reduced to modelling the $\overline{\rho'\cdot\vec{u}''}$ correlation. Much work has been done on this model, for instance by Jones [12] who introduces a first gradient assumption for this quantity. We will here only use the first gradient hypothesis already applied for the turbulent heat flux closure.

Starting from the state equation and a first gradient assumption for the heat flux, we obtain the following relations:

$$\overline{\rho'\vec{u}''} = -\frac{\overline{\rho\theta''\vec{u}''}}{\bar{T}}$$

with

$$-\overline{\rho\vec{u}''\theta''} = \frac{\mu_t}{Prt}\overrightarrow{\operatorname{grad}}\,\bar{T};$$

then

$$G_k = -\frac{\mu_t}{Prt\cdot\bar{\rho}^2}\,\overrightarrow{\text{grad}}\,\bar{\rho}\cdot\overrightarrow{\text{grad}}\,\bar{P}.$$

For the classical Boussinesq approximation $\overrightarrow{\text{grad}}\,\bar{P}\approx\bar{\rho}\cdot\vec{g}$, then using the Reynolds decomposition for velocity and temperature and the first gradient hypothesis, the term G_k is reduced to:

$$G_k = -\frac{\mu_t}{Prt\cdot\bar{\rho}}\,\overrightarrow{\text{grad}}\,\bar{\rho}\cdot\vec{g}.$$

A term similar to G_k can be introduced for the ε evolution equation by writing P_ε and D_ε in the form [13]

$$P_\varepsilon = C_{\varepsilon 1}\frac{\varepsilon}{k}\left(P_k+\frac{G_k}{\bar{\rho}}\right);\quad D_\varepsilon = C_{\varepsilon 2}\cdot\frac{\varepsilon^2}{k}.$$

The value P_ε can be corrected to take into account a preferred production direction [14, 15], then we write

$$P_\varepsilon = C_{\varepsilon 1}\frac{\varepsilon}{k}\left(P_k+\frac{G_k}{\bar{\rho}}\right)(1+C_{\varepsilon 3}R_f)$$

where

$$R_f = -\overline{G(w''^2)}\Big/\left(P_k+\frac{G_k}{\bar{\rho}}\right)\quad\text{and}\quad G(\overline{W''^2})$$

is the energy production for the vertical velocity component.

2.4. *Closed system of equations*

The modellisation is made at high Reynolds number and small Mach number, then the terms $\overline{\varphi}$, $\overline{p'\,\text{div}\,\vec{u}''}$ and $\overline{\text{div}\,\vec{u}''p'}$ are negligible. The term $\partial\bar{P}/\partial t$ is also supposed to be negligible, compared with $\bar{\vec{U}}\,\overrightarrow{\text{grad}}\,\bar{P}$. Then we have the final system of equations in non-dimensional form

$$\frac{\partial\bar{\rho}}{\partial t}+\text{div}\left(\bar{\rho}\bar{\vec{U}}\right)=0$$

$$\frac{\partial}{\partial t}\bar{\rho}\bar{\vec{U}}+\text{div}\left(\bar{\rho}\bar{\vec{U}}*\bar{\vec{U}}\right)$$

$$=-\overrightarrow{\text{grad}}\,\bar{P}-\frac{2}{3Re}\overrightarrow{\text{grad}}\left(\text{div}\,\bar{\vec{U}}\right)$$

$$+\frac{1}{Re}\text{div}\left[\overrightarrow{\overrightarrow{\text{grad}}}\,\bar{\vec{U}}+\overrightarrow{\overrightarrow{\text{grad}}}^{t}\bar{\vec{U}}\right]$$

$$+\text{div}\left[\frac{1}{Rt}\left(\overrightarrow{\overrightarrow{\text{grad}}}\,\bar{\vec{U}}+\overrightarrow{\overrightarrow{\text{grad}}}^{t}\bar{\vec{U}}\right)\right]$$

$$-\overrightarrow{\text{grad}}\left[\frac{2}{3}\left(\bar{\rho}\cdot k+\frac{1}{Rt}\text{div}\,\bar{\vec{U}}\right)\right]+\frac{\bar{\rho}}{Fr}\frac{\vec{g}}{|\vec{g}|}$$

$$\bar{\rho}\left[\frac{\partial\bar{T}}{\partial t}+\bar{\vec{U}}\,\overrightarrow{\text{grad}}\,\bar{T}\right]$$

$$=\text{div}\left[\frac{1}{Rt\,Prt}\overrightarrow{\text{grad}}\,\bar{T}+\frac{1}{Re\,Pr}\overrightarrow{\text{grad}}\,\bar{T}\right]$$

$$+Ec\left[\bar{\vec{U}}\,\overrightarrow{\text{grad}}\,\bar{P}-\xi\right]$$

$$\bar{\rho}\frac{\partial k}{\partial t}+\bar{\rho}\,\bar{\vec{U}}\cdot\overrightarrow{\text{grad}}\,k$$

$$=\text{div}\left[\left(\frac{1}{Re}+\frac{1}{Rt\cdot\sigma_k}\right)\overrightarrow{\text{grad}}\,k\right]$$

$$+\bar{\rho}\cdot P_k+\xi-\bar{\rho}\cdot\varepsilon$$

$$\bar{\rho}\frac{\partial\varepsilon}{\partial t}+\bar{\rho}\,\bar{\vec{U}}\cdot\overrightarrow{\text{grad}}\,\varepsilon$$

$$=\text{div}\left[\left(\frac{1}{Re}+\frac{1}{Rt\cdot\sigma_\varepsilon}\right)\overrightarrow{\text{grad}}\,\varepsilon\right]$$

$$+\bar{\rho}\cdot P_\varepsilon-C_{\varepsilon 2}\bar{\rho}\frac{\varepsilon^2}{k}$$

$$\bar{\rho}(\alpha\bar{T}+1)=1;\quad\text{with}\quad\alpha=\frac{T_p-T_\infty}{T_\infty}$$

$$P_k=\frac{1}{\bar{\rho}}\left(\frac{1}{Rt}\left(\overrightarrow{\overrightarrow{\text{grad}}}\,\bar{\vec{U}}+\overrightarrow{\overrightarrow{\text{grad}}}^{t}\bar{\vec{U}}\right)-\frac{2}{3}\left(\bar{\rho}\cdot k+\frac{1}{Rt}\text{div}\,\bar{\vec{U}}\right)\vec{I}\right)\overrightarrow{\overrightarrow{\text{grad}}}\,\bar{\vec{U}}$$

$$\xi=-\frac{1}{\bar{\rho}^2\cdot Rt\cdot Prt}\overrightarrow{\text{grad}}\,\bar{\rho}\cdot\overrightarrow{\text{grad}}\,\bar{P}$$

$$Re=\rho_\infty\frac{\delta U_\infty}{\mu};\quad Fr=\frac{U_\infty^2}{\delta g};\quad Pr=\frac{\mu_\infty C_p}{\lambda_\infty};$$

$$Ec=\frac{(\gamma-1)M_\infty^2 T_\infty}{T_p-T_\infty};\quad\frac{1}{Rt}=c_\mu\bar{\rho}\frac{k^2}{\varepsilon}=\frac{\mu_t}{\mu_\infty}$$

$$M_\infty=\frac{U_\infty}{C};\quad\gamma=\frac{C_p}{C_v}.$$

Model constants are those used in incompressible flow, see Table 1.

2.5. *Modifications to the standard model to take into account the gravity effects*

As we have seen, the turbulent viscosity used in the k–ε model is a scalar which cannot take into account

Table 1.

$C_{\varepsilon 1}$	$C_{\varepsilon 2}$	$C_{\varepsilon 3}$	σ_k	σ_ε
1.44	1.92	0.8	1.0	1.3

the influence of a strongly anisotropic phenomenon such as gravity. One possible solution to this problem is to use second order turbulence models which do not include any turbulent viscosity assumptions (ASM or RSM model). However, these models are difficult to use and require the use of adapted calculation algorithms. We have decided here to use these second order models and particularly the ASM model in order to obtain information for improving the standard k–ε model.

Considering the classical relation leading to the Rodi algebraic model [16]

$$(\text{Conv}-\text{diff})_{\overline{\overline{w''^2}}} = \frac{\overline{\overline{w''^2}}}{k}(\text{Conv}-\text{diff})_k$$

written for the w component parallel to gravity forces.

Starting from this relation, Rodi [16] determines an expression for C_μ in the following form:

$$C_\mu = \omega \cdot \frac{\overline{\overline{w''^2}}}{k}$$

$$\omega = \frac{1-C_2+\frac{3}{2}C_2 \cdot C_2' \cdot f \cdot Q(\beta, f, \alpha) \cdot L(P_k, G_k)}{C_1+\frac{3}{2}C_1' \cdot f}$$

where (with $\mathbb{G}_k = G_k/\bar{\rho}$)

$$Q(\beta, f, \alpha) = \frac{1-\dfrac{(1-C_3)(1-C_{2T}) \cdot \alpha(R, B, f) \cdot B}{(1-C_2+\frac{3}{2}C_2 \cdot C_2' \cdot f)C_{1T}}}{1+\dfrac{(1-C_3)B}{(C_1+\frac{3}{2}C_1' \cdot f)C_{1T}}}$$

$$L(P_k, G_k) = \frac{0.09}{2(1-C_2)\left(C_1-1+C_2\left(\dfrac{P_k+\mathbb{G}_k}{\varepsilon}\right)\right)}{3C_1\left(C_1+\dfrac{P_k+\mathbb{G}_k}{\varepsilon}-1\right)}$$

and

$$\frac{\overline{\overline{w''^2}}}{k} = \frac{2}{3}\frac{C_1-1+\dfrac{P_k+\mathbb{G}_k}{\varepsilon}F_1+\dfrac{\mathbb{G}_k}{\varepsilon}F_2}{C_1+2C_1' \cdot f+\dfrac{P_k+\mathbb{G}_k}{\varepsilon}-1}$$

$$F_1 = C_2-2C_2C_2' \cdot f$$

$$F_2 = 3-C_2-2C_3+2 \cdot C_2 \cdot C_2' \cdot f$$

$$\alpha(R, B, f) = \frac{1}{C_{1T}+C_{1T}' \cdot f+2(1-C_{3T})R \cdot B}$$

$$B = \beta \cdot g\frac{k^2}{\varepsilon^2}\frac{\partial T}{\partial Z}.$$

In our study, we have used the relation given by Chung and Sung [17] for f, which is the wall damping

$$f = \frac{k^{3/2}(1-R_f)^{1/4}}{C_w \cdot Z \cdot \varepsilon}$$

where $(1-R_f)^{1/4}$ is the buoyancy correction factor, and Z is the distance from the wall.

The values of constants are given in Table 2.

These relations make it possible to take into account the gravity effects in the expression of C_μ since the calculation of $\overline{\overline{w''^2}}$ includes the G_k production term. Several models may be used for the turbulent Prandtl number. The first is based on Rodi's work [16] and consists of writing

$$Prt_R = \frac{\omega}{\alpha}$$

where

$$\alpha = \frac{1}{C_{1T}+C_{1T}' \cdot f+2(1-C_{3T})R \cdot B}.$$

A second approach deduced from experimental work carried out by Munk and Anderson [18] and dealing with the study of stratified marine medium, can be used to write

$$Prt_E = Prt_0 \cdot \frac{(1+3.33Ri)^{1.5}}{(1+10Ri)^{0.5}}$$

with

$$R_i = -\frac{g}{T}\frac{\partial T/\partial Z}{(\partial U/\partial Z)^2}$$

(R_i = Richardson's gradient number),

Prt_0 is the value of the turbulent Prandtl number, in the absence of stratification (here taken equal to one).

Rodi's approach [16] makes it possible to introduce both the gravity and wall effects, whereas Munk and Anderson's approach [18] consists of introducing the gravity term more explicitly through Richardson's gradient number.

In order to take into account the wall effects, we have substituted in Munk's approach Prt_R given by Rodi [16] for Prt_0, then the present proposition is to write:

$$Prt = Prt_R \cdot \frac{(1+3.33R_i)^{1.5}}{(1+10R_i)^{0.5}}.$$

2.6. *Treatment of zones close to boundaries*

Equations for the k–ε model were developed for high Reynolds number flows. They can therefore not be used for zones very close to boundaries in which viscous effects become important.

Local equilibrium equations then have to be used, making it possible to transfer the condition at the boundary to a distance at which viscous effects become negligible.

The semi-logarithmic law normally used is that which is obtained analytically for a turbulent isothermal boundary layer established on a flat plane. However, it would appear that this law remains applicable for flows in which high temperature variations exist [19]. In this case, the values of Karman's kinematic k_u and thermal k_θ constants in the logarithmic law should be changed in order to take into account the degree of stratification or heat flux variations at

Table 2.

$C_{\varepsilon 1}$	$C_{\varepsilon 2}$	$C_{\varepsilon 3}$	σ_k	σ_ε	C_1	C_2	C_3
1.44	1.92	0.8	1.0	1.3	1.8	0.6	0.6
C'_1	C'_2	C_{1T}	C_{2T}	C_{3T}	C'_{1T}	R	C_w
0.6	0.3	3.0	0.5	0.5	0.5	1.0	3.72

the boundary. For a stable stratification, results provided by various authors [17, 20] give values of k_u between 0.13 and 0.42 and values of k_θ between 0.1 and 0.46. In our experience, the values of these constants are between 0.13 and 0.24 for k_u, and between 0.1 and 0.2 for k_θ. Based on the experimental data that we used to validate the model, we added variations to the constant for the kinematic law; the experimentally determined flux is imposed at the wall.

2.7. *Solution method and boundary conditions*

The discretization scheme is semi-implicit in time, allowing linearization of equations at each time step. The momentum equation coupled with the continuity equation is solved by an Uzawa type iterative procedure together with a conjugated gradients method [21].

The spatial discretization is based on a finite element variational formulation, the details of which are described by Brun [22].

On solid boundaries, non-homogeneous Dirichlet type conditions are imposed on all variables except for the temperature for which a Neuman type condition is applied.

Concerning free boundaries, Dirichlet type conditions are imposed at the start of the calculation range and at the outside boundary for all variables. At the end of the calculation range, homogeneous Neuman conditions are imposed for all variables except the pressure for which a reference condition is fixed (for example, atmospheric pressure).

3. EXPERIMENTAL STUDY OF A THERMALLY STABLE STRATIFIED TURBULENT BOUNDARY LAYER

3.1. *Experimental set up*

The wind tunnel used is of "closed loop" type with venting downstream of the test section. This test section is 14 m long, 3.7 m wide and 2.5 m high. The roof is adjustable in order to maintain constant pressure in the direction of flow.

The following are arranged at the entrance of the test section:

(i) a 0.17 solidity homogenization grid;
(ii) a wall air injection device for enhancing the boundary layer thickness; and
(iii) a comb for fixing the transition of the boundary layer.

Stable thermal stratification is obtained by intense cooling of the floor with liquid nitrogen: a complete discription is given by Morel *et al.* [23].

The flow velocity is continuously adjustable from 1 m s^{-1} to 10 m s^{-1}.

3.2. *Measurement technique*

The mean and fluctuating kinematic and thermal fields are explored using a T.S.I. three wire probe comprising two 5 μm diameter platinum wires crossed and connected to a constant temperature anemometric system; these two wires are located on each side of a 2 μm diameter platinum wire through which a low current passes, sensitive to temperature only. Sensitivity coefficients are obtained by direct calibration in a wind tunnel in which velocity can be adjusted between 0.5 and 3 m s^{-1} and temperature can be adjusted from -20 to $+30$°C.

Temperature and flux measurements at the wall are carried out by copper–constantan thermocouples distributed over the entire surface of the floor.

Data acquisition and processing are carried out by a PDP 11/73 computer.

4. COMPARISON BETWEEN PREDICTION AND EXPERIMENT

Several series of tests were carried out on a smooth wall, firstly in a neutral situation and secondly in a stable thermally stratified situation, with an external flow velocity U_∞ of 1.80 m s^{-1}.

The main results of these tests have been presented elsewhere [23], and we will compare these results with those provided by the model proposed in this paper. The entry profiles to start the calculation are experimental profiles of:

(i) the mean velocity;
(ii) the mean temperature;
(iii) the turbulent kinetic energy; and
(iv) the calculated dissipation of the turbulent viscosity within the $X = 6.4$ m section, where the origin is fixed at the transition comb. Experimental turbulent heat fluxes are imposed at the wall together with kinematic Karman constant values k_u.

We made comparisons between experimental and numerical results at section $X = 9300$ mm (which represents a good compromise between the end effects of

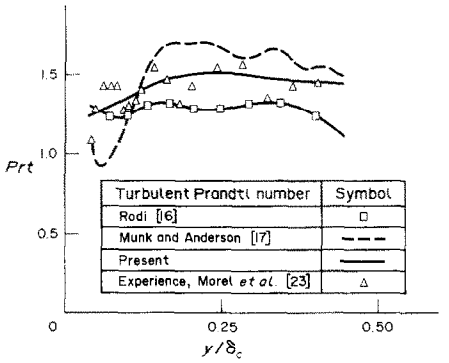

FIG. 1. Turbulent Prandtl number profiles.

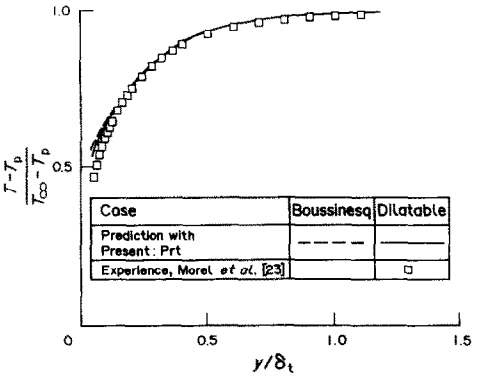

FIG. 3. Mean temperature profiles.

the working section and development of a steady state. The following two cases were examined:

Case (a)—classical Boussinesq hypothesis (variations of ρ are only included in the gravity term of the momentum equation.

Case (b)—fully dilatable flow (variations of ρ taken into account in all terms).

In both of these cases, we have used successively a constant turbulent Prandtl number and a variable turbulent Prandtl number, keeping respectively Rodi [16], Munk and Anderson's [18] formulation and the relation proposed in this study, that we will designate by 'present' *Prt*. The profiles of the different turbulent Prandtl numbers in terms of the boundary layer thickness δ_c are shown in Fig. 1. It can be seen that the 'present' Prandtl is the best representation of the experimental results obtained.

Non-dimensional distributions of mean velocity and temperature (Figs. 2 and 3) obtained experimentally agree fairly well with model results, regardless of which case is considered, except close to the wall ($Z/\delta < 0.15$) where the predicted temperature is higher than the experimental results.

Concerning turbulence characteristics, we will examine each of the two cases (a) and (b) separately using the different choices for the turbulent Prandtl number.

The turbulent heat fluxes $\overline{w\theta}/U_*(T_s - T_p)$ are presented for cases (a) and (b) on Figs. 4 and 5, respectively. For case (a), the present relation proposed for the turbulent Prandtl number is the only one that agrees with experimental results except in the internal layer in which a difference remains. In case (b), regardless of what relations are used for the turbulent Prandtl number, except for the constant turbulent Prandtl number, the results obtained agree fairly well with experimental results. Note that the model with proposed 'present' *Prt* gives quasi-similar results in cases (a) and (b), however with a better prediction for case (b) close to the wall.

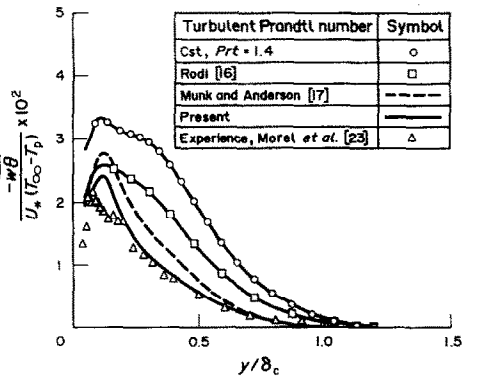

FIG. 4. Distribution of vertical turbulent heat flux. Case (a)—Boussinesq hypothesis.

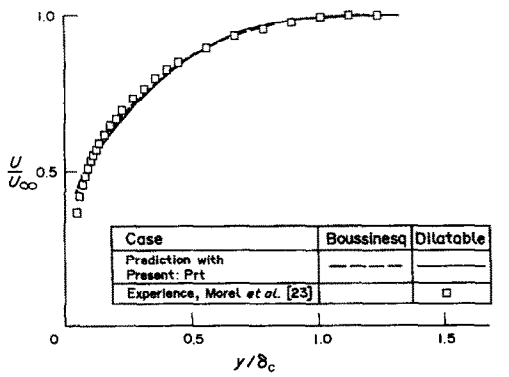

FIG. 2. Mean velocity profiles.

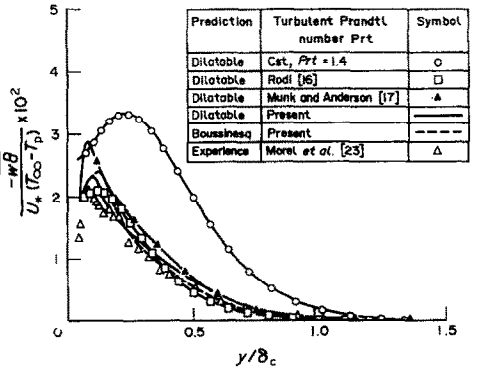

FIG. 5. Distribution of vertical turbulent heat flux (dilatable flow).

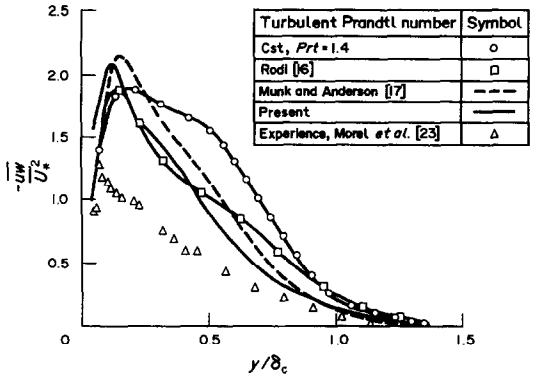

FIG. 6. Square root of Reynolds stress. Case (a)—Boussinesq hypothesis.

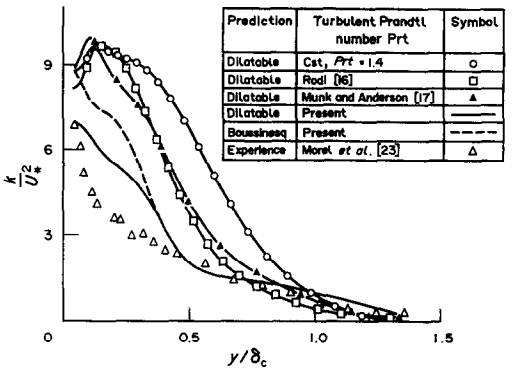

FIG. 9. Distribution of turbulent kinematic energy (dilatable flow).

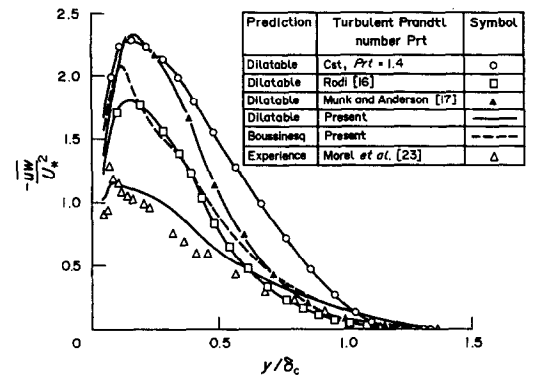

FIG. 7. Square root of Reynolds stress (dilatable flow).

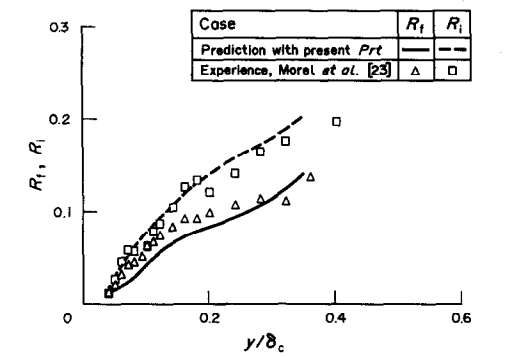

FIG. 10. Distribution of Richardson gradient and flux number.

The Reynolds stress $\overline{uw}/U_*^2$ are given in Figs. 6 and 7. Only the model with the 'present' (Prt) for case (b) gives results close to experimental results in the dilatable case.

The turbulent kinetic energy (Figs. 8 and 9) is satisfactorily predicted within the $Z/d > 0.4$ zone for cases (a) and (b) with the proposed (Prt), however, case (b) gives a slightly better approach in the internal zone.

In case (b) the proposed model predicts fairly well the gradient R_i and flux R_f Richardson's numbers, as shown in Fig. 10.

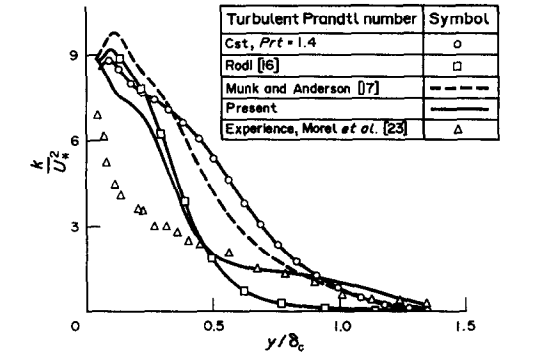

FIG. 8. Distribution of turbulent kinematic energy. Case (a)—Boussinesq hypothesis.

5. CONCLUSION

It would appear that buoyancy effects are not satisfactorily taken into account by Munk and Anderson's empirical relation [18]. However, it should be emphasized that the result given by Munk and Anderson [18] was established for a marine medium. The formulation of the turbulent Prandtl number by Rodi [16] deduced from the A.S.M. model offers an advantage to Munk's relation. But in this formulation the introduction of the wall damping function f, which takes into account the influence of the wall, presents rather an inconvenience due to its empirical character. Despite fairly encouraging results provided by the model used here, it is still necessary to search for further improvement in the wall region in which there are significant differences from experimental results. An attempt should therefore be made to find a specific empirical relation for a stable stratified boundary layer in order to improve the prediction for the entire layer.

REFERENCES

1. S. P. S. Arya, Buoyancy effects in a horizontal flat-plate boundary layer, *J.F.M.* **68**, 321–343 (1975).
2. C. A. G. Webster, An experimental study of turbulence in a density stratified shear flow, *J.F.M.* **19**, 221–245 (1964).

3. Y. Ogawa, P. G. Diosey, K. Uehara and H. Ueda, Wind tunnel for studying the effects of thermal stratification in the atmosphere, *Atmos. Environ.* **115,** 807–821 (1981).
4. S. Komori, H. Ueda, F. Ogino and T. Mizushimat, Turbulence structure in stably stratified open chanel flow, *J.F.M.* **130,** 13 (1983).
5. M. Wier und N. Römer, Experimentelle Untersuchung von stabil und instabil geschichten turbulenten plattengrenzschichten mit bodenrauhigkeit, *Z. Flugwiss. Weltroumforsh.* **11,** 75 (1987).
6. V. Lienhard and C. W. Van-Atta, Decay of turbulence in thermally stratified flow, *J.F.M.* **210,** 57–112 (1990).
7. J. C. R. Hunt and W. H. Snyder, Experiments on stably and neutrally stratified flow over a model three dimensional hill, *J.F.M.* **96,** 671–704 (1980).
8. W. P. Jones and J. J. McGuirk, Mathematical modelling of gas-turbine combustion chambers, AGARD CP 275 (1979).
9. B. E. Launder and D. B. Spalding, The numerical computation of turbulent flows. In *Computer Methods in Applied Mechanics and Engineering*, pp. 269–283. North-Holland, Amsterdam (1974)
10. K. Hanjalic and B. E. Launder, A Reynolds stress model of turbulence and its application to thin shear flow, *J.F.M.* **52,** 609 (1972).
11. J. Lumley and H. Tennekes, *A First Course in Turbulence*. MIT Press, Cambridge, MA (1973).
12. W. P. Jones and J. M. Whitelaw, Prediction of turbulent reacting flows in practical systems, ASME ENSMP 106643 (1981).
13. B. I. Davidov, *Sov. Phys. Dokl.* **6,** 10 (1961).
14. M. S. Hossain and W. Rodi, Mathematical modelling of vertical mixing in stratified channel flow, *Proc. 2nd Int. Symp on Stratified Flows*, Trondheim, Norway (1980).
15. P. Bradshaw, Effects of streamline curvature on turbulent flow, *Agardograph* No. 169 (1973).
16. W. Rodi, *Turbulent Buoyant Jet and Plumes*. Pergamon Press, Oxford (1984).
17. M. K. Chung and H. J. Sung, Four-equation turbulence model for prediction of the turbulent boundary layer affected by buoyancy force over a flat plate, *Int. J. Heat Mass Transfer* **27,** 2387–2395 (1984).
18. W. M. Munk and E. R. Anderson, Notes on the theory of thermocline, *J. Marine Res.* **1** (1948).
19. R. K. Cheng and T. T. Ng, Some aspects of strongly heated turbulent boundary layer flow, *Physics Fluids* **25,** 1333–1341 (1982).
20. B. B. Petukhov, A. F. Polyakov and Yu. V. Tsypulev, Peculiarities of non-isothermal turbulent flows in horizontal flat channels at low Reynolds number and under significant buoyancy forces, *2nd Symposium on Turbulent Shear Flow*, Imperial College, London, Vol. 9, pp. 11 16 (1979).
21. M. Buffat, Etude de la simulation numérique par une méthode d'éléments finis des écoulements internes subsoniques instationnaires bi et tridimensionnels, Thèse esscience Université Claude Bernard Lyon (1991).
22. G. Brun, Developpement et application d'une méthode d'éléments finis pour le calcul des écoulements turbulents fortement chauffés, Thèse E.C.L. (1988).
23. R. Morel, E. Alcaraz, M. Ayrault, R. Zegadi and P. Mejean, Effects of thermal stable stratification on turbulent boundary layer characteristics, *Atmos. Environ.* **25,** 1263–1269 (1991).

VALIDATION D'UN MODELE k–ε A PARTIR DE RESULTATS EXPERIMENTAUX EN COUCHE LIMITE TURBULENTE THERMIQUEMENT STRATIFIEE STABLE

Résumé—Un modèle de turbulence 2D (k–ε) est développé dans le cadre d'écoulements dilatables à grands nombres de Reynolds. Une nouvelle approche concernant la modélisation du terme de corrélation densité-vitesse est proposée et une relation concernant le nombre de Prandtl turbulent tenant compte à la fois des effets de paroi et de gravité a été utilisée. Ce modèle a été validé au moyen de résultats expérimentaux obtenus au laboratoire de Mécanique des fluides et d'Acoustique de l'E.C.L. sur un écoulement de couche limite turbulente thermiquement stratifiée stable se développant sur une paroi plane lisse fortement refroidie.

BEWERTUNG EINES k–ε MODELLES DURCH AN EINER THERMISCH STABIL GESCHICHTETEN TURBULENTEN GRENZSCHICHT ERHALTENE EXPERIMENTELLE ERGEBNISSE

Zusammenfassung—Ein zweidimensionales k–ε Turbulenzmodell in ausdehnbaren Strömungen mit hoher Reynolds-Zahl wurde entwickelt. Eine neue Annäherung für die Modellierung der Dichte-Geschwingkeit Korrelation und eine für die turbulente Prandtl-Zahl gleichzeitig die Auswirkung der Wand und der Schwerkraft berücksichtigende Formel wurden vorgeschlagen. Dieses Modell wurde mittels der im Labor für Strömungsmechanik und Akustik, an einer thermisch stabil geschichtenten turbulenten Grenzschicht längs einer stark abgekühlten glatten ebenen Wand erhaltenen Ergebnisse nachgeprüft.

ПРОВЕРКА ЭФФЕКТИВНОСТИ k–ε МОДЕЛИ С ПОМОЩЬЮ ЭКСПЕРИМЕНТАЛЬНЫХ ДАННЫХ ДЛЯ ТЕРМИЧЕСКИ УСТОЙЧИВОГО СТРАТИФИЦИРОВАННОГО ТУРБУЛЕНТНОГО ПОГРАНИЧНОГО СЛОЯ

Аннотация—Разработана двумерная (k–ε) модель турбулентности для расширяющихся течений при больших числах Рейнольдса. Предложен новый подход для моделирования слагаемого, устанавливающего корреляцию между плотностью и скоростью. Использовано соотношение для турбулентного числа Прандтля с учетом эффектов стенки и силы тяжести. Эффективность разработанной модели проверялась с помощью экспериментальных данных, полученных в лаборатории Центральной Лионской школы механики жидкостей и акустики для термически устойчивого стратифицированного турбулентного пограничного слоя, развивающегося при быстром охлаждении гладкой граничной поверхности.